Dynamical properties of Sb- and Bi-covered (110) surfaces of III-V compounds

2002 J. Phys.: Condens. Matter 14 5865

(http://iopscience.iop.org/0953-8984/14/24/301)

INSTITUTE OF PHYSICS PUBLISHING JOURNAL OF PHYSICS: CONDENSED MATTER

J. Phys.: Condens. Matter **14** (2002) 5865–5879 PII: S0953-8984(02)34756-8

Dynamical properties of Sb- and Bi-covered (110) surfaces of III–V compounds

Jürgen Fritsch[1], **Alexander Dvořák, Marcus Arnold and Ulrich Schröder**

Institut für Theoretische Physik, Universität Regensburg, D-93040 Regensburg, Germany

E-mail: juergen.fritsch@physik.uni-regensburg.de

Received 12 March 2002
Published 31 May 2002
Online at stacks.iop.org/JPhysCM/14/5865

Abstract

We present results from plane-wave pseudopotential calculations and density-functional perturbation theory applied to investigate the surface phonon dispersion of (110) surfaces of InAs and InP covered by monolayers of Sb and Bi. The importance of vibrational spectroscopy for the investigation of structural properties is demonstrated for the Bi-covered InAs(110) surface which forms a (1×1) and, in addition, a (1×2) phase. Our calculations predict two prominent low-frequency modes which are fingerprints of the missing-row reconstruction recently proposed for the (1×2) phase. A comparison of the modes allows us to analyse systematic trends and to study the physical origin of vibrational states occurring on clean and adsorbate-covered III–V(110) surfaces. The electronic band structure computed for the (1×1) and (1×2) phases of the Bi-covered InAs(110) surface is in agreement with experimental data. Compared with the (1×1) phase, we find a much smaller band gap for the (1×2) reconstruction.

(Some figures in this article are in colour only in the electronic version)

1. Introduction

The adsorption of the group-V semimetals Sb and Bi on (110) surfaces of III–V semiconductors attracts much attention both experimentally and theoretically. Epitaxial overlayers with well-ordered (1×1) symmetry can be produced by the deposition of Sb on GaAs, GaP, InAs and InP(110) [1–5]. Therefore, a large number of measured data are available for these systems from low-energy electron diffraction (LEED), surface-extended x-ray adsorption fine-structure (SEXAFS), photoemission diffraction (PED) and grazing-incidence x-ray diffraction (GIXD) [3, 6–12] studies. The adsorption of Bi on III–V(110) surfaces leads to (1×1) overlayers only on substrates with a sufficiently large lattice constant like InP,

[1] Author to whom any correspondence should be addressed.

InAs, GaSb [8, 13–16], while missing adatom layers occur for Bi deposited on materials like GaAs. Recently, the formation of another ordered structural phase with (1×2) periodicity was observed for the adsorption of Bi on some of the III–V(110) surfaces. Particular attention was paid to Bi:InAs(110)(1×2) [17–19] and Bi:GaSb(110)(1×2) [15, 20, 21].

It is generally accepted that the (1×1) phase of Sb and Bi adsorbed on III–V(110) surfaces can be explained in terms of the epitaxial continued layer (ECL) structure proposed by Skeath *et al* [22]. According to the ECL model, two group-V atoms are adsorbed per unit cell of the pristine surface, occupying all atomic positions of the 'next lattice layer' derived from the symmetry of the underlying material. By this, the adatoms are arranged in chains along the $[1\bar{1}0]$ direction. In a series of total-energy calculations mainly performed for Sb adsorbed on GaAs, GaP, InAs and InP [23–29], the ECL geometry was found to be the most favourable structure. In addition, the relaxation parameters and the zone-centre frequencies of highly localized surface vibrations computed for the ECL structure [27–29] compare very well with experimental data [7, 9, 10, 30–32].

In contrast with the common agreement on the ECL model for the (1×1) phase, further experimental and theoretical work is needed to understand in more detail the (1×2) reconstruction additionally observed for Bi adsorbed on GaSb and InAs(110). Measurements based on x-ray diffraction, scanning tunnelling microscopy (STM) and photoelectron spectroscopy provide evidence that the Bi:GaSb(110)(1×2) reconstruction can be described by the modified epitaxial continued layer (MECL) structure which is characterized by missing III–V rows in the first substrate layer and a complete monolayer (ML) coverage with tilted Bi zigzag chains oriented parallel to the $[1\bar{1}0]$ direction [15]. The MECL model is also supported by density-functional calculations carried out for the (1×1) and (1×2) phases of Bi:GaSb(110) [33]. The structural parameters and electronic bands computed for the MECL geometry, which has the lowest total energy, compare very well with experimental data [15, 16].

More recently, the structural parameters of Bi:InAs(110)(1×2) as well as the electronic density of states and band structure have been determined by means of GIXD [19] and ultraviolet photoemission spectroscopy (UPS) [14, 17]. For an interpretation of the electronic band structure measured for the (1×2) phase, De Renzi and co-workers have used the results from total-energy calculations performed to investigate the (1×1) ECL geometry [34]. However, further theoretical studies have to be carried out to add to previous work [34, 35], in order to fully understand the structural and electronic details of the Bi:InAs(110)(1×2) reconstruction.

Here, we report the results from density-functional calculations carried out to determine the relaxation parameters and vibrational modes of Sb and Bi adsorbed in the ECL structure on the (110) surfaces of InP and InAs. In addition, we discuss the equilibrium positions, electronic states and vibrational modes computed for Bi adsorbed in the (1×2) MECL geometry on InAs(110). Our density-functional calculations are carried out on the basis of a plane-wave molecular-dynamics approach [36], the full-potential linearized augmented-plane-wave (FP-LAPW) method [37] and within density-functional perturbation theory (DFPT) [38, 39] applied to periodically repeated thin crystal films.

By analysing the vibrational states of Sb and Bi on the III–V(110) surfaces, the structure of the adsorption systems can be studied thoroughly. In particular for the MECL geometry of the Bi:III–V(110)(1×2) phase, characteristic surface phonon modes occur. They provide a clear identification of the missing-row reconstruction, in which the Bi zigzag chains are bonded exclusively either to substrate anions or cations.

The phonon modes of the covered surfaces are also very useful for explaining in more detail the vibrational features of the clean surfaces. As an example, we discuss the bond-length-conserving rotational mode predicted by the tight-binding total-energy calculations of

Wang and Duke for the pristine (110) surfaces [40]. Theoretical studies, which accounted for the coupling of surface states with bulk phonons, showed that the rotational mode is largely resonant with bulk vibrations. Hence, no clear identification of this mode was possible [43–47]. Recent DFPT calculations have demonstrated that epitaxial overlayers of Sb atoms can significantly reduce the phonon frequency of the rotational mode and its coupling to bulk states [29]. Therefore, it is microscopic for Sb:GaAs(110) and Sb:GaP(110). However, it is still resonant for Sb adsorbed on InAs and InP(110). The present investigation confirms the prediction obtained on the basis of the mass approximation that the rotational mode tends to become a true surface mode in the case of Bi deposition [29].

The paper is organized as follows. Section 2 illustrates the computational details of our theoretical investigations. Section 3 presents the main results obtained for Bi adsorbed in the ECL structure on InAs and InP(110), including a comparison with the respective Sb adsorption systems. Section 4 is focused on the structural, electronic and vibrational states of the (1×2) phase of Bi:InAs(110). Our results are summarized in section 5.

2. Theoretical method

Our computations are carried out in the framework of density-functional theory [48] applied in the local-density approximation (LDA) [49]. For the exchange–correlation potential we use the form proposed by Ceperley and Alder [50] in the parametrization suggested by Perdew and Zunger [51]. Sb monolayers on InAs and InP(110) are investigated by means of plane-wave pseudopotential calculations as described in detail in [29]. To study Bi adsorbed on the III–V(110) surfaces, we use the *ab initio* molecular-dynamics package *fhi98md* [36] and norm-conserving separable pseudopotentials [52–54] generated on the basis of the neutral-atom valence electron configuration for In, As, P and the configuration $[Xe]5d^{10}6s^{2}6d^{3}$ for Bi. In addition, the In 4d electrons are taken into account by means of the non-linear core correction [55]. The plane-wave cut-off energies are 25 Ryd for Bi:InAs(110) and 30 Ryd for Bi:InP(110). The accuracy of the plane-wave pseudopotential approach is checked by supplementary calculations carried out for Bi:InAs(110) on the basis of the FP-LAPW method [37].

We study the (110) surfaces of periodically repeated thin crystal films, fixing the lattice constant at the theoretical value determined for the bulk. Our computations yield $a = 5.921$ Å and $a = 6.086$ Å for InP and InAs, in good agreement with the experimental data $a = 5.869$ Å and $a = 6.036$ Å taken from [39].

For the (1×1) phase of Sb and Bi adsorbed on InAs and InP(110), we consider thin crystal films containing a total of nine atomic layers with 18 atoms per unit cell. The slabs comprise seven substrate layers and one ML of Sb or Bi adsorbed on either of their two surfaces. The Bi:InAs(110)(1×2) reconstruction is described in terms of non-symmetric slabs that contain seven InAs layers with a total of 13 pairs of In and As atoms, four Bi atoms and four H atoms per unit cell. In the first substrate layer, which is terminated by a complete ML of Bi atoms, every other row of III–V atoms is missing. The dangling bonds of the opposite surface of the crystal films are saturated by the H atoms.

Two neighbouring crystal films are separated by a distance which is equal to three removed atomic (110) layers. The thickness of the slabs and their separation guarantee that the interaction of neighbouring crystal films is negligible and that the surfaces of each slab are sufficiently decoupled. For the $\boldsymbol{k}$-point sampling we use six special points in the case of the (1×1) phase and four special points for the (1×2) reconstruction.

The equilibrium positions of the adsorbed group-V atoms and those of the substrate are determined by minimizing the total energy with the help of the Hellmann–Feynman forces,

starting the atomic relaxation from positions derived from the symmetry of the bulk. For the (1×1) phase each atom is allowed to move with the exception of the central-layer atoms, while for the (1×2) reconstruction the two InAs layers and their H termination in the lower region of the slabs are kept at fixed positions. The relaxation is stopped when the forces are smaller than 0.1 mRyd au^{-1}. This defines the computed equilibrium positions with a numerical uncertainty of $<$0.01 Å.

To study the vibrational features of the adsorption systems, dynamical matrices of entirely relaxed crystal films are computed. For Bi on InAs and InP, we use the direct approach by calculating successively the Hellmann–Feynman forces resulting from the positive and negative displacement of each individual atom in the unit cell by 0.042 Å from the equilibrium position along the three Cartesian directions. This allows us to determine the dynamical matrix at the $\overline{\Gamma}$ point of the surface Brillouin zone (SBZ). In order to identify resonances and deeply penetrating surface states of the ECL adsorption systems, we construct the dynamical matrices of larger slabs comprising 25 atomic layers. The force constants in the surface region of the large crystal films are assumed to be the same as the respective force constants in the nine-layer slabs. For the inner region of the large crystal films, we use bulk force constants. In the case of the Sb-covered surfaces, complete phonon dispersion curves along the $\overline{\Gamma X}$ and $\overline{\Gamma X'}$ directions are determined by means of DFPT using the formalism of Baroni and co-workers [38, 39]. Details of these calculations are summarized in [29].

3. Adsorption in the ECL structure

Room temperature deposition of Sb and Bi on III–V(110) surfaces starts with the formation of a two-dimensional ML, followed by the growth of three-dimensional islands at higher coverages. In the limit of 1 ML, the adsorbed atoms form a well-ordered overlayer with (1×1) periodicity. Several structural models were proposed for the (1×1) phase. A detailed compilation of experimental and theoretical work done to determine the surface geometry of the (1×1) adsorption system is given in [28]. In view of the large number of measured and computed data, it is well established by now that the one-monolayer deposition of Sb and Bi on the (110) surfaces of III–V semiconductors results in the ECL structure proposed by Skeath *et al* [22].

3.1. Relaxation of the ECL structure

Figure 1 illustrates the equilibrium positions of the relaxed (1×1) ECL geometry of Sb and Bi adsorbed on InAs or InP(110). The structural parameters determined for these systems are summarized in table 1. The relaxation parameters were determined by means of plane-wave pseudopotential computations as described in [29] in the case of the Sb-covered surfaces and on the basis of *ab initio* molecular-dynamics calculations for the adsorption of Bi.

Additionally, we have determined the relaxation of Bi:InAs(110)(1×1) by means of the FP-LAPW method [37] within the LDA [56] for the exchange–correlation potential. In these calculations, the muffin-tin radii were chosen as $R_{\mathrm{MT}}(\mathrm{Bi}) = 2.4$, $R_{\mathrm{MT}}(\mathrm{In}) = 2.4$ and $R_{\mathrm{MT}}(\mathrm{As}) = 2.0$ (in au) for Bi, In and As. The wavefunctions were expanded in plane waves up to 12.25 Ryd and a maximal angular momentum of $l_{\max} = 10$. For the potential, a maximal cut-off energy of 100.0 Ryd was used. The data obtained within the FP-LAPW approach and those from the plane-wave calculations agree very well, as can be seen from table 1. The agreement shows that the pseudopotential approach allows us to describe Bi overlayers on InAs and InP with high accuracy.

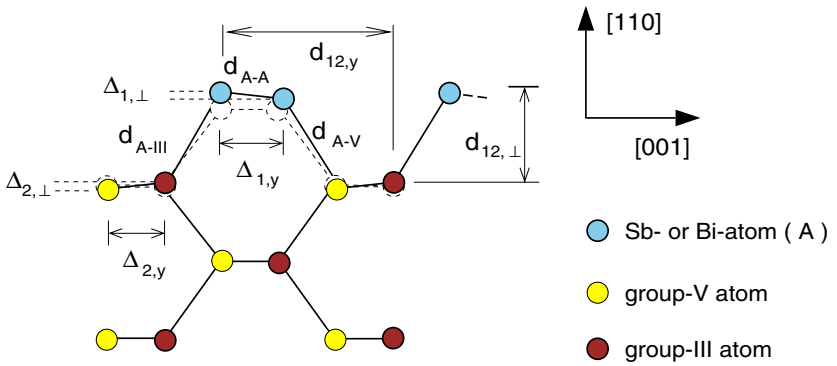

Figure 1. A side view of the relaxed ECL structure of Sb or Bi adatoms (A) covering the (110) surface of III–V semiconductors. The structural parameters determined for the adsorption on InAs and InP(110) are summarized in table 1.

Table 1. Relaxation parameters (in Å) of the ECL structure of Sb and Bi adsorbed on the (110) surfaces of InAs and InP. The parameters are defined in figure 1. For Bi:InAs(110), we compare results obtained from pseudopotential plane-wave calculations (PP-PW) with those determined on the basis of the FP-LAPW method.

System	Method	ω_1	ω_2	$\Delta_{1,\perp}$	$\Delta_{2,\perp}$	$d_{12,\perp}$	$d_{\mathrm{A-III}}$	$d_{\mathrm{A-V}}$	$d_{\mathrm{A-A}}$
Bi:InAs(110)	FP-LAPW	4.1°	2.2°	0.15	0.06	2.51	2.85	2.71	2.98
Bi:InAs(110)	PP-PW	4.9°	4.2°	0.18	0.11	2.52	2.87	2.73	3.00
Sb:InAs(110)	PP-PW	4.7°	4.0°	0.16	0.11	2.41	2.77	2.62	2.87
Bi:InP(110)	PP-PW	5.7°	3.2°	0.21	0.09	2.50	2.86	2.64	2.98
Sb:InP(110)	PP-PW	5.8°	3.8°	0.20	0.10	2.43	2.77	2.52	2.84

The data listed in table 1 also compare very well with results from other DFT calculations for Sb:III–V(110) [27, 28] and Bi:III–V(110) surfaces [34] as well as with experimental data from [8–10]. As can be seen from figure 1, the relaxation of the clean (110) surfaces is removed by the adsorption of Sb or Bi and replaced by a slight counter-rotation of the anion–cation chains in the first substrate layer. The adlayer chains formed by the overlayer atoms are tilted in a similar way to the first-layer zigzag chains of the respective clean surfaces. However, the relaxation angle of the adsorption layer is distinctly smaller.

Characterized by only slightly tilted adatom zigzag chains oriented along the $[1\bar{1}0]$ direction, the Sb- and Bi-covered surfaces can be compared very well with each other. The magnitude of the tilt angle essentially reflects the difference between the adatom–anion and adatom–cation bond lengths. This can be seen from the parameters $\Delta_{1,\perp}$, $d_{\mathrm{A-V}}$ and $d_{\mathrm{A-III}}$. The covalent radii of Sb and Bi are 1.40 and 1.46 Å. Consistent with this, the Bi–III, Bi–V and Bi–Bi bonds are about 0.9–0.14 Å longer than the respective Sb–III, Sb–V and Sb–Sb bonds. However, compared with those for Sb the interatomic distances involving Bi turn out to be larger than estimated solely from the covalent radii.

3.2. Vibrational modes of the ECL structure

Apart from small differences observed for the details of the relaxation, the adsorption geometry is essentially the same for Bi and Sb deposited in the (1×1) phase on the III–V(110) surfaces of InAs and InP. Also the bonding structure and thus the interatomic force constants compare well

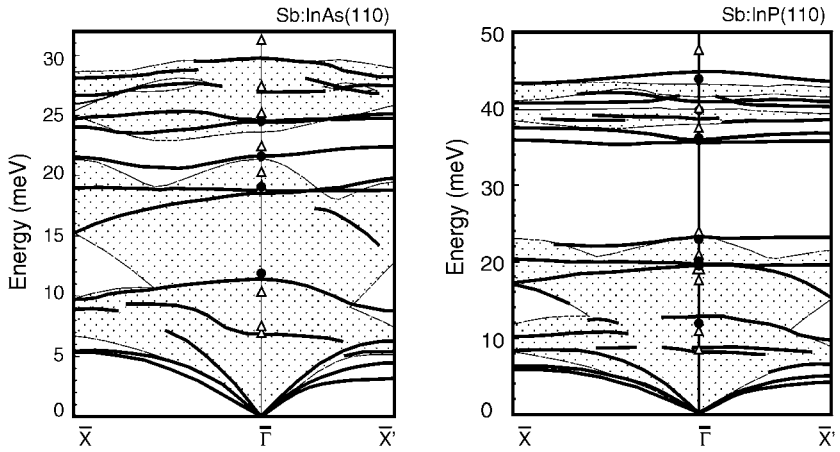

Figure 2. Phonon dispersion computed for the (1 × 1) ECL adsorption structure of Sb on InAs and InP(110). Surface-localized modes are indicated by solid curves. Triangles: frequencies determined in the frozen-phonon calculation of [27]. Filled circles: experimental data from Raman spectroscopy [30, 32].

Table 2. Vibrational frequencies (in meV) of zone-centre phonon modes of Sb and Bi adsorbed on InAs and InP(110). The corresponding displacement patterns are illustrated in figure 3.

System	A_1'	A_2'	A_3'	A_1''	A_2''
Sb:InAs(110)	21.7	24.5	29.9	18.7	24.6
Sb:InP(110)	23.0	35.9	44.7	19.4	35.5
Bi:InAs(110)	15.0	22.7	28.7	13.5	25.4
Bi:InP(110)	15.4	34.6	43.6	13.7	39.2

with each other. Therefore, the surface phonon modes of the individual adsorption systems mainly reflect the different masses of the substrate and the adlayer atoms.

Figure 2 illustrates the phonon dispersion of Sb:InAs(110) and Sb:InP(110) calculated by means of DFPT for the $\overline{\Gamma X}$ direction along the adlayer zigzag chains and for the $\overline{\Gamma X'}$ direction perpendicular to the surface chains. The triangles and filled circles indicate the results from the plane-wave pseudopotential calculations of [27] and vibrational frequencies measured by Raman spectroscopy [30, 32]. A detailed discussion of the phonon modes is given in [29].

At the $\overline{\Gamma}$ point, five vibrational modes were found to be abundant in all Sb:III–V(110) adsorption systems [29]. These modes are illustrated in figure 3. The total number of surface-localized modes, however, depends on the particular mass ratios that characterize the individual adsorption systems. As an example, the rotational mode originally discussed by Wang and Duke [40] for the clean (110) surfaces is microscopic only for Sb on GaAs and GaP(110), while it is resonant for Sb adsorbed on InAs and InP(110). In this context, two important questions arise:

(i) Are the five common modes of the Sb adsorption systems also present in Bi:InAs(110) and Bi:InP(110); and
(ii) is the rotational mode resonant or microscopic for Bi adsorbed in the ECL geometry on InAs and InP(110)?

Table 2 summarizes the frequencies of the five modes that indeed turn out to be microscopic also for the adsorption of Bi on InAs and InP(110). The vibrational energies of the A_1' and A_1''

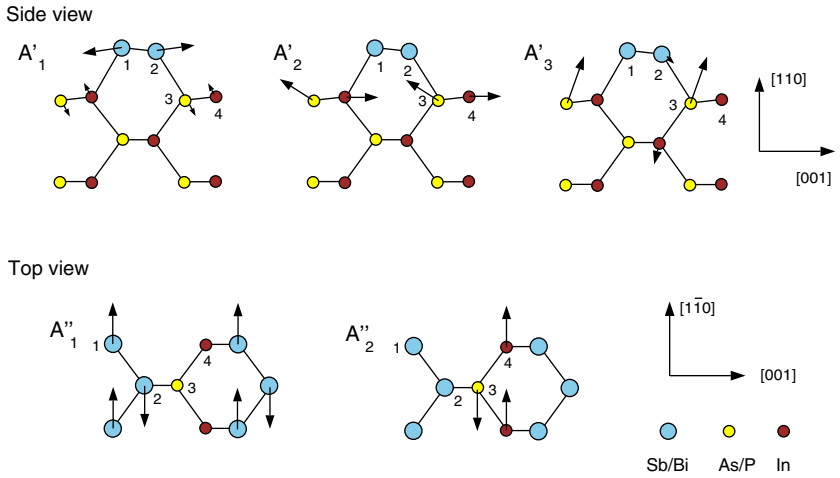

Figure 3. Side and top views of zone-centre phonon displacement patterns characteristic for Sb and Bi adsorbed in the ECL structure on InAs and InP(110). Corresponding atoms in the top and side views are numbered. The frequencies of the modes are summarized in table 2.

modes directly reflect whether Sb or Bi atoms are adsorbed, while the substrate atoms have only a minor influence. This behaviour can be explained by the eigenvectors which clearly show that the modes are dominated by oscillations of the adatoms and only small displacements of the atoms in the layers below. The frequencies of the individual Sb modes are larger by a factor of 1.39–1.49 compared with the those of the Bi overlayer. Interestingly, the mass difference between the Bi and Sb atoms gives only a factor ranging around $\sqrt{m_{\mathrm{Bi}}/m_{\mathrm{Sb}}} \approx 1.31$. This indicates that the bond strengths in the overlayer and between the overlayer and the substrate are slightly reduced for Bi in comparison with Sb. This observation is consistent with the fact that the bond lengths in the Bi adsorption system are somewhat larger than simply derived from the covalent radii of Bi and Sb.

The frequencies of the A_2', A_3' and A_2'' modes change only to a small extent when Bi is adsorbed instead of Sb. The phonon energies are significantly larger for InP(110), indicating that these modes are localized in the substrate. Figure 3 shows that the modes are dominated by oscillations in the first substrate layer. While the frequencies of the A_2'' modes are larger in the Bi adsorption systems, the energies of the other two modes are smaller in Bi:InAs(110) and Bi:InP(110) in comparison with the Sb-covered surfaces. Consistent with this, the adlayer atoms take part in the A_2' and A_3' modes with appreciable vibrational amplitudes, while they are at rest in the A_2'' modes.

On the one hand, there are three microscopic first-substrate-layer modes. However, on the other hand, only two modes with dominant vibrations in the adsorption layer occur, namely the phonon states A_1' and A_1''. The corresponding third mode of the adlayer should be characterized by atomic displacements mainly normal to the surface. This is the rotational mode which is resonant for Sb on InAs and InP(110) [29]. It is also not possible to identify this mode for the Bi-covered InAs(110) surface. However, in the case of Bi adsorbed on InP(110), we can identify the rotational mode with a vibrational energy of 7.5 meV. Its eigenvector is illustrated in figure 4.

The comparison of our results obtained for the clean as well as the Sb- and Bi-covered (110) surfaces of a number of III–V semiconductors shows unambiguously that the rotational mode of the clean surfaces and for some of the adsorption systems lies in a spectral region

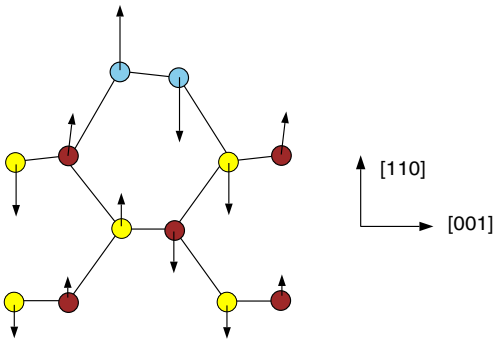

Figure 4. The displacement pattern of the rotational mode in Bi:InP(110) in a side view of the first four atomic layers.

which has a high density of bulk states. The strong hybridization with substrate vibrations changes its displacement pattern drastically, so it is impossible to identify the rotational mode. Its frequency can be effectively tuned by changing the atomic masses in the surface region. On covering the (110) surfaces with heavy adatoms in the ECL structure, the rotational mode finally becomes localized.

In addition to the vibrational features discussed so far, two more modes are present in the ECL adsorption structure of Bi on InAs and InP(110). One of these states has A′ symmetry. It is dominated by a stretching oscillation of the Bi–In back-bonds, accompanied by smaller vibrations the other atoms in the surface region. The phonon energies are 17.4 meV for Bi:InAs(110) and 18.3 meV for Bi:InP(110). The displacement pattern of the other mode has A″ symmetry. It is characterized by an in-phase oscillation of the first-layer substrate atoms along the chain direction having an energy of 5.8 and 6.9 meV for Bi adsorbed on InAs and InP(110).

4. Adsorption in the (1 × 2) phase

Annealing of thick Bi layers on III–V(110) surfaces results in the desorption of the semimetal atoms with the exception of the first ML. Besides the (1 × 1) phase, that can be prepared at moderate temperatures, an additional structural phase with (1 × 2) periodicity develops at elevated temperatures in the case of Bi adsorbed on InAs(110) [17–19] and GaSb(110) [15, 20, 21].

Photoemission experiments indicate metallic behaviour for the Bi:InAs(110)(1 × 2) phase, while the (1 × 1) adsorption structure has a clear gap [14, 18]. In a recent experiment based on angle-resolved ultraviolet photoemission spectroscopy (ARUPS), De Renzi and co-workers have investigated the occupied surface-state bands of the (1 × 2) phase of Bi on InAs(110). They discuss their results by means of a comparison with theoretical data from *ab initio* calculations for the (1 × 1) ECL geometry.

The (1 × 2) reconstruction of Bi deposited on III–V(110) surfaces was also investigated by means of GIXD [15, 19] and STM [15]. The results are interpreted in terms of the MECL structure, in which every other III–V row in the first substrate layer is missing. Compared with other surface geometries, the model of the missing-row reconstruction was found to give the lowest surface energy for the Bi:GaSb(110)(1 × 2) surface. Analogously, our calculations indicate that MECL structure has the lowest surface energy also for the Bi:InAs(110)(1 × 2) phase, which is favoured by 0.14 eV per (1 × 2) unit in comparison with the ECL geometry.

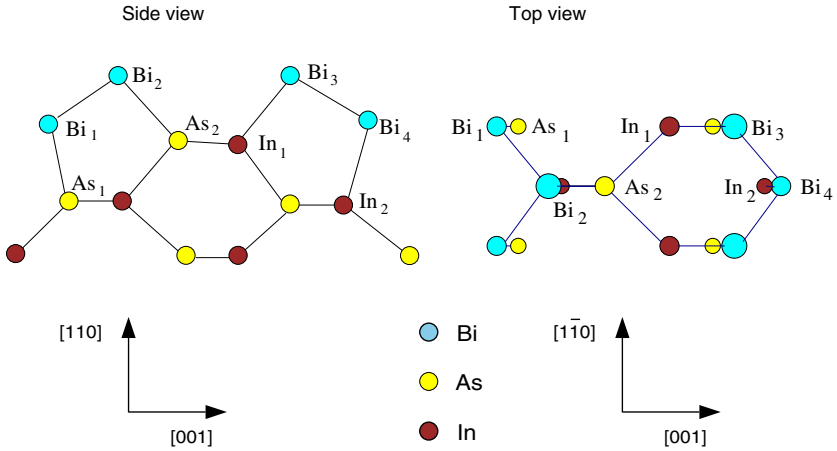

Figure 5. Atomic positions of the MECL structure of Bi adsorbed on InAs(110). Corresponding atoms in the top and side views are numbered.

4.1. Relaxation of the MECL structure

Figure 5 illustrates the MECL structure, in which the number of Bi atoms per unit area is the same as in the ECL geometry. The adlayer atoms still form covalently bonded zigzag chains along the [1$\bar{1}$0] direction on the surface. However, every other chain of III–V atoms in the first substrate layer is missing in comparison with the ECL structure. The rebonding established in the MECL geometry leads to purely anion-bonded and purely cation-bonded Bi chains. The Bi chains are substantially tilted with respect to the horizontal orientation since they are attached to first- and second-substrate-layer atoms.

Table 3 summarizes bond lengths computed for the (1×2) MECL adsorption structure and compares our data with results obtained from GIXD measurements for Bi:InAs(110)(1×2) [19] and density-functional calculations carried out by Gay and Srivastava to study Bi:GaSb(110)(1×2) [33]. Included also are our data for the ECL geometry, which indicate that individual bond lengths are only slightly changed in the (1×2) phase. A comparison of the numbers listed in the table shows two obvious trends:

(i) the interatomic separation in the anion-bonded Bi chains is larger than that of the cation-bonded chains; and
(ii) the back-bond lengths of the upper Bi atoms are consistently smaller than those of the lower Bi atoms.

The Bi zigzag chains are strongly tilted with respect to the horizontal orientation, because of the missing-row structure. Hence, a substantial vertical separation $\Delta_{i,j}$ between the Bi atoms i and j is observed. We obtain $\Delta_{1,2} = 1.29$ Å and $\Delta_{3,4} = 1.24$ Å, to be compared with 1.21 and 1.06 Å measured by means of GIXD [19] as well as with 1.16 and 1.30 Å computed for Bi:GaSb(110)(1×2) [33].

4.2. Electronic states of the MECL structure

The electronic band structure of the ECL adsorption geometry is well understood, because of the wealth of experimental and theoretical data available for (1×1) overlayers of Sb and Bi on III–V(110) surfaces. In contrast with that, only a few experimental and theoretical investigations have been carried out so far to study the surface electronic states of the Bi:III–V(110)(1×2)

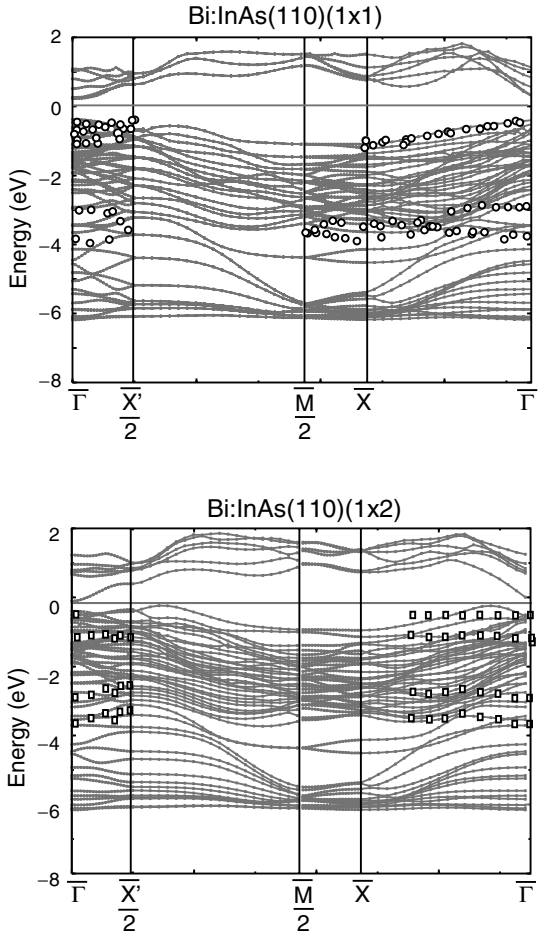

Figure 6. Electronic dispersion of the Bi:InAs(110) ECL and Bi:InAs(110) MECL surface structure. Data from angle-resolved photoemission spectroscopy for the (1×1) phase [13] and the (1×2) phase [17] are indicated by circles and squares. For a direct comparison, the dispersion of the (1×1) structure is folded in accord with the SBZ of the (1×2) geometry.

Table 3. Bond lengths (in Å) determined for the MECL adsorption structure of Bi on InAs(110) in comparison with measured data from GIXD [19], results from DFT calculations for Bi:GaSb(110)(1×2) [33] and our results obtained for the ECL (1×1) adsorption structure. The atom numbers are explained in figure 5. A_i^s and C_i^s refer to substrate anions and cations.

System	Reference	Bi_1–Bi_2	Bi_3–Bi_4	Bi_1–A_1^s	Bi_2–A_2^s	Bi_3–C_1^s	Bi_4–C_2^s
Bi:InAs, MECL	Present	3.05	3.01	2.74	2.71	2.87	2.93
Bi:InAs, MECL	[19]	2.98	2.93	2.98	2.62	3.05	3.10
Bi:GaSb, MECL	[33]	2.99	2.98	2.89	2.86	2.64	2.66
Bi:InAs, ECL	Present	3.00	3.00	2.73	2.73	2.87	2.87

systems [14, 16–18, 33]. Interestingly, photoemission spectroscopy experiments indicate that the phase transition from the (1×1) to the (1×2) reconstruction is accompanied by a transition from semiconducting to metallic behaviour [14, 18].

Figure 6 illustrates the electronic dispersion of thin crystal films terminated in the (1×1) and (1×2) Bi adsorption reconstruction. For a direct comparison, the electronic states of the (1×1) phase were computed by using a slab unit cell having the same dimensions as that used to describe the MECL structure. This corresponds to folding back the dispersion of the (1×1) phase into the SBZ of the (1×2) reconstruction.

Because of the large number of atoms per unit cell, there are many electronic branches. The majority of the bands correspond to bulk states which are similar in the (1×1) and (1×2) phases. However, the comparison shows marked differences for the states in the gap region, which can therefore be identified as surface features. In particular, the agreement with the experimental data from ARUPS for Bi:InAs(110)(1×1) [13] is very good. In addition to the electronic states close to the valence band edge, two additional branches are seen by experiment and theory in the folded dispersion at about -3 and -4 eV.

The ARUPS experiments of De Renzi *et al* [17] carried out to study Bi:InAs(110)(1×2) resolve two flat branches at about -3 and -4 eV that are consistent with our computations. More interestingly, the ARUPS measurements detect two flat branches along the $\overline{\Gamma}\overline{\mathrm{X}}$ direction at about -0.3 and -0.9 eV. One key problem in the interpretation of the experimental data was the lack of information on the number of electronic states that have to be expected. Therefore, five Gaussian curves were used to analyse the photoemission spectra in terms of four surface states and one strong bulk feature. While the electronic states resolved at about -4, -3 and -0.9 eV are reasonably reproduced by our calculation, significant deviations occur for the branch at -0.3 eV. Our computations give an indication of two electronic states close to the valence band edge which correspond to the dangling bonds of the Bi atoms attached to the In atoms of the first and second substrate layers. To fit the experimental data, however, only one Gaussian curve was used in this energy region. Since the contribution to the intensity in the photoemission spectra is very small in this part of the spectrum, the measurement of the electronic dispersion near the Fermi level might be very challenging.

Our (1×1) crystal films exhibit an energy gap of about 0.6 eV. In the (1×2) phase, however, the valence band has a maximum close to the $\overline{\mathrm{X}}'/2$ point, while the first branch of the conduction band has a low-lying minimum at the $\overline{\Gamma}$ point. Therefore, the MECL structure is characterized by a small indirect gap of only 0.14 eV. Although our calculations give a clear reduction of the band gap, the MECL structure is still semiconducting. By means of the FP-LAPW approach [37], we were also able to examine the effects of spin–orbit coupling. Interestingly, spin–orbit coupling does not change the electronic dispersion of the Bi adsorption system, although it is known to be responsible for substantial changes in the electronic states in the bulk of Bi. For an interpretation of the experimental observations [14,17], it might be necessary to take into account finite-temperature effects. At a temperature of 570 K, the Fermi smearing results in an average electronic population of the lowest conduction band of about 20%.

4.3. Vibrational modes of the MECL structure

The open bonding structure of the MECL geometry with its missing III–V rows in the first substrate layer and the purely anion- and cation-bonded Bi zigzag chains is reflected in a series of characteristic surface-localized vibrational features. We have investigated the surface dynamics of Bi:InAs(110)(1×2) by diagonalizing the dynamical matrix determined for the zone centre within the direct approach by calculating the coupling constants from the Hellmann–Feynman forces computed for a total of 204 off-equilibrium geometries. Since the MECL structure has mirror symmetry with respect to the $(1\bar{1}0)$ plane, the vibrational states are strictly separated into A′ modes with atomic oscillations exclusively in the $(1\bar{1}0)$ plane and A″ modes with atomic motions only along the $[1\bar{1}0]$ direction.

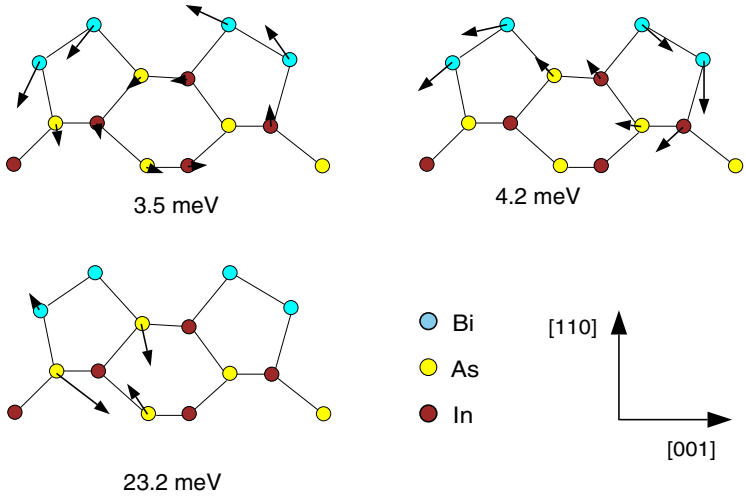

Figure 7. Side views of phonon displacement patterns of three vibrational states that are characteristic for the MECL (1 × 2) adsorption structure.

All of the A″ modes of the (1 × 2) system can be clearly related to vibrational features of the ECL geometry. The A″ phonon at 5.8 meV of the (1 × 1) phase has two corresponding states in the (1 × 2) reconstruction. They are dominated by in-phase vibrations of the atoms in the first-substrate-layer III–V chains parallel to the chain direction. In the state at 6.4 meV, the vibrations are mainly restricted to the first substrate layer, while appreciable in-phase oscillations of the second-substrate-layer atoms in the opposite direction occur in addition in the mode at 6.3 meV. The A_1'' phonon of the (1 × 1) surface at 13.5 meV has two counterparts in the (1 × 2) system: we find one mode with opposing oscillations of the As-bonded Bi atoms along the chain direction with an energy of 13.2 meV and one mode at 13.4 meV with atomic oscillations essentially restricted to the cation-bonded Bi chains. The A_2''-phonon state of the (1 × 1) surface with an energy of 25.4 meV has a corresponding vibration in the (1 × 2) system at an energy of 25.7 meV. This mode is characterized by an out-of-phase oscillation of the remaining atoms in the first substrate layer along the chain direction.

Also a number of A′ states of the (1 × 1) phase, namely those occurring at 15.0, 17.4 and 28.7 meV, can be directly related to vibrational states of the (1 × 2) reconstruction. The A′ mode of the MECL geometry having an energy of 15.0 meV is similar to the 15.0 meV feature of the ECL structure. It has the character of bond-stretching vibrations of the atoms in each Bi chain with displacements perpendicular to the $[1\bar{1}0]$ direction and in the planes defined by the individual adlayer zigzag chains. As for the ECL phase, a stretching oscillation of the Bi–In back-bond appears in the (1 × 2) surface at a slightly higher frequency of 18.4 meV. It is dominated by atomic motions of the upper Bi atoms and their first-substrate-layer bonding partners. Finally, the mode of the ECL structure at 28.7 meV is related to a similar oscillation of the first-substrate-layer As atoms with an energy of 27.3 meV.

The three modes illustrated in figure 7 do not directly correspond to any zone-centre vibrational state of the (1 × 1) phase. In the mode at 23.2 meV, mainly the As atoms of the outermost three substrate layers are moving. The probably most characteristic vibrational features of the (1 × 2) MECL structure are the two low-frequency A′ modes at 3.5 and 4.2 meV. They are dominated by a rotation-like motion of the Bi atoms and the other atoms of the fivefold

rings formed by the adlayer and the outermost two substrate layers about the centres of the rings. In the mode at 3.5 meV, neighbouring rings are moving in phase, while the state at 4.2 meV shows an opposing oscillation of the rings.

The rotational modes can be compared with the $A_4'(\overline{X'})$ state illustrated in figure 9 of [29] for the Sb-covered surfaces, which has a phonon energy of 3.1 meV for Sb:InAs(110). Since the $\overline{X'}$ point of the (1×1) phase corresponds to the $\overline{\Gamma}$ point of the (1×2) structure, the $A_4'(\overline{X'})$ phonon has to be compared with the A' mode at 4.2 meV. However, because of the larger mass of Bi and the slightly reduced force constants of the back-bonds, the respective mode should have an energy significantly smaller than 3.0 meV. The larger frequency of the 4.2 meV mode and also that of its partner at 3.5 meV are a consequence of the particular geometry of the MECL structure with its missing III–V rows. In addition, the adlayer atom displacements of the two modes have large z-components because of the large tilt angle of the zigzag chains in the MECL structure, while the adatoms are moving mainly parallel to the surface in the respective phonon mode of the ECL phase. With their particular frequencies and displacement patterns the two modes can be regarded as fingerprints of the missing-row reconstruction. They can be very useful for the identification of the MECL structure of Bi:InAs(110)(1×2) and analogously for that of Bi:GaSb(110)(1×2) by means of vibrational spectroscopy.

5. Summary

We have presented the results from plane-wave pseudopotential calculations for the structural, electronic and vibrational properties of the Sb- and Bi-covered (110) surfaces of InAs and InP. Besides the (1×1) ECL geometry, which is known to be formed by the adsorption of Sb and Bi, we have investigated the (1×2) phase that is observed in addition for the deposition of Bi on the (110) surfaces.

The ECL structure of the Sb-covered surfaces has been investigated by a large number of experiments. Our results obtained for Sb:InAs(110) and Sb:InP(110) are in good agreement with the measured data. In particular, the vibrational features determined by means of DFPT compare very well with results from Raman spectroscopy. This indicates that our *ab initio* calculations are able to describe the atomic structure and the bond strengths of the ECL geometry with high accuracy. In the same way, epitaxial Bi overlayers adsorbed in the (1×1) phase form the ECL structure on the III–V(110) surfaces considered here. The relaxed atomic positions are similar to those of Sb overlayers. A comparison with results from additionally performed computations based on the FP-LAPW method shows that the structural and electronic properties of Bi adsorption layers can be described very well within the plane-wave pseudopotential approach. The vibrational frequencies determined for Bi deposited in the (1×1) phase on InAs and InP(110) reflect that the main difference between the ECL geometry of Bi overlayers and that of Sb overlayers consists in the much larger atomic mass of Bi. In addition, a slight weakening of the force constants of the adlayer and the back-bonds is found for Bi-covered surfaces in comparison with Sb coverages. Our calculations give clarifying information about the rotational mode, which was originally discussed for the clean surfaces on the basis of tight-binding calculations [40]. Its frequency can be effectively tuned by changing the atomic masses in the surface region. The rotational mode is found to be microscopic for Bi adsorbed on InP(110), while it is resonant for the Bi:InAs(110) surface. This conclusively shows that hybridization with bulk vibrations makes it difficult to identify the rotational mode as a microscopic surface phonon especially on clean III–V(110) surfaces [29, 40, 43].

Finally, we have investigated the atomic, electronic and vibrational properties of the (1×2) reconstruction of Bi adsorbed on InAs(110). The MECL structure recently suggested by van Gemmeren *et al* [15] for Bi:GaSb(110)(1×2) is found to have a lower surface energy in

comparison with the ECL geometry. The equilibrium positions calculated for the missing-III–V-row reconstruction are in good agreement with data from GIXD measurements [19] and results obtained within DFT for Bi:GaSb(110)(1 × 2) [33].

The electronic band structure computed for the (1 × 1) and (1 × 2) phases of the Bi-covered InAs(110) surface is compared with data from angle-resolved photoemission spectroscopy [13, 17]. The agreement is very good in both cases. However, for the electronic states of the (1 × 2) structure close to valence band edge our results differ from the measured data. In particular, photoemission spectroscopy indicates metallic behaviour, while the calculations give a small indirect band gap of 0.14 eV for the (1 × 2) phase.

A large number of microscopic phonon modes are found for the (1 × 2) missing-row reconstruction. Many of the vibrational features of the MECL structure can be related to modes of the (1 × 1) phase. In addition, a pair of phonon modes occur, that are clear fingerprints of the missing-row reconstruction. They are characterized by rotational oscillations of the fivefold rings formed by the adsorbed Bi zigzag chains and the atoms of the first and second substrate layer below. The measurement of the corresponding zone-centre frequencies of 3.5 and 4.2 meV would provide clear evidence for the MECL structure.

References

[1] Esser N, Zahn D R T, Müller C, Richter W, Stephens C, Whittle R, McGovern I T, Kulkarni S and Braun W 1992 *Appl. Surf. Sci.* **56–9** 169

[2] Nowak C, Chassé A, Hempelmann A, Richter W, Dudzik E, Whittle R, McGovern I T, Braun W and Zahn D R T 1994 *Surf. Sci.* **307–9** 685

[3] Nowak C, Hempelmann A, Märkl A, Chassé A, Dudzik E, Müller C, McGovern I T, Braun W, Richter W and Zahn D R T 1995 *Surf. Sci.* **331–3** 564

[4] Nowak C, Krujatz J, Märkl A, Meyne C, Chassé A, Braun W, Richter W and Zahn D R T 1995 *Surf. Sci.* **331–333** 619

[5] Patrin J C, Li Y Z, Chander M and Weaver J H 1992 *Phys. Rev.* B **46** 10 221

[6] Ford W K, Guo T, Lantz S L, Wan K, Chang S L, Duke C B and Lessor D L 1990 *J. Vac. Sci. Technol.* B **8** 940

[7] Ford W K, Guo T, Lessor D L and Duke C B 1990 *Phys. Rev.* B **42** 8952

[8] Ford W K, Guo T, Wan K-J and Duke C B 1992 *Phys. Rev.* B **45** 11 896

[9] Nowak C 1990 *PhD Thesis* Berlin University of Technology

[10] Nowak C, Chassé A, Braun W, Richter W, McGovern I T and Zahn D R T 1996 *J. Electron Spectrosc. Relat. Phenom.* **80** 143

[11] Miyano K E, Woicik J C, Kendelewicz T, Spicer W E, Richter M and Pianetta P 1993 *Phys. Rev.* B **47** 6444

[12] Betti M G, Mariani C, Jedrecy N, Pinchaux R, Ruocco A and Sauvage-Simkin M 1994 *Phys. Rev.* B **50** 14 336

[13] McIlroy D N, Heskett D, Swanston D M, McLean A B, Ludeke R, Munekata H, Prietsch M and DiNardo N J 1993 *Phys. Rev.* B **47** 3751

[14] Betti M G, Corradini V, del Pennino U, De Renzi V, Fantini P and Mariani C 1998 *Phys. Rev.* B **58** R4231

[15] van Gemmeren T *et al* 1998 *Phys. Rev.* B **57** 3749

[16] McIlroy D N, Heskett D, McLean A B, Ludeke R, Munekata H and DiNardo N J 1993 *Phys. Rev.* B **48** 11 897

[17] De Renzi V, Betti M G, Mariani C, Almeida J and Grioni M 2000 *J. Phys.: Condens. Matter* **12** 7721

[18] De Renzi V, Betti M G, Corradini V, Fantini P, Martinelli V and Mariani C 1999 *J. Phys.: Condens. Matter* **11** 7447

[19] Betti M G, Berselli D, Mariani C, Jedrecy N, Sauvage-Simkin M, Garreau Y and Pinchaux R 1999 *Phys. Rev.* B **59** 15 760

[20] van Gemmeren T, Lottermoser L, Falkenberg G, Bunk O, Johnson R L, Feidenhansl R L and Nielsen M 1998 *Surf. Sci.* **414** 254

[21] van Gemmeren T and Johnson R L 1995 *Surf. Sci.* **331–3** 613

[22] Skeath P, Lindau I, Su C Y and Spicer W E 1981 *J. Vac. Sci. Technol.* B **19** 556

[23] LaFemina J P 1992 *Surf. Sci. Rep.* **16** 133

[24] Srivastava G P 1993 *J. Phys.: Condens. Matter* **5** 4695

[25] Srivastava G P 1993 *Phys. Rev.* B **47** 16 616
Srivastava G P 1994 *Surf. Sci.* **307–9** 328

[26] Schmidt W G, Wenzien B and Bechstedt F 1994 *Phys. Rev.* B **49** 4731
Schmidt W G, Wenzien B and Bechstedt F 1994 *Surf. Sci.* **307–9** 235
[27] Schmidt W G and Srivastava G P 1995 *Surf. Sci.* **331–3** 540
[28] Schmidt W G, Bechstedt F and Srivastava G P 1996 *Surf. Sci. Rep.* **25** 141
[29] Fritsch J, Arnold M and Schröder U 2000 *Phys. Rev.* B **61** 16 682
[30] Hünermann M 1990 *PhD Thesis* Aachen University of Technology, Germany
Hünermann M, Geurts L and Richter W 1991 *Phys. Rev. Lett.* **66** 640
[31] Esser N, Köpp M, Haier P and Richter W 1993 *J. Electron Spectrosc. Relat. Phenom.* **64/65** 85
[32] Esser N, Köpp M, Haier P and Richter W 1995 *Phys. Status Solidi* a **152** 191
[33] Gay S C A and Srivastava G P 2000 *Phys. Rev.* B **61** 2688
[34] Umerski A and Srivastava G P 1995 *Phys. Rev.* B **51** 2334
[35] Gay S C A, Çakmak'M and Srivastava G P 2000 *Surf. Sci.* **454–6** 26
[36] Bockstedte M, Kley A, Neugebauer J and Scheffler M 1997 *Comput. Phys. Commun.* **107** 187
[37] Blaha P, Schwarz K and Luitz J 1997 *WIEN97* Vienna University of Technology
This is an improved and updated Unix version of the original copyrighted WIEN code, which was published by
Blaha P, Schwarz K, Sorantin P and Trickey S B 1990 *Comput. Phys. Commun.* **59** 399
[38] Baroni S, Giannozzi P and Testa A 1987 *Phys. Rev. Lett.* **58** 1861
[39] Giannozzi P, de Gironcoli S, Pavone P and Baroni S 1991 *Phys. Rev.* B **43** 7231
[40] Wang Y R and Duke C B 1988 *Surf. Sci.* **205** L755
[41] Harten U and Toennies J P 1987 *Europhys. Lett.* **4** 833
[42] Doak R B and Nguyen N B 1987 *J. Electron Spectrosc. Relat. Phenom.* **44** 205
[43] Fritsch J, Pavone P and Schröder U 1993 *Phys. Rev. Lett.* **71** 4194
[44] Fritsch J, Pavone P and Schröder U 1995 *Phys. Rev.* B **52** 11 326
[45] Eckl C, Fritsch J, Pavone P and Schröder U 1997 *Surf. Sci.* **394** 47
[46] Fritsch J, Eckl C, Pavone P and Schröder U 1997 *Festkörperprobleme (Advances in Solid State Physics)* vol 36, ed R Helbig (Braunschweig: Vieweg) p 135
[47] Fritsch J and Schröder U 1999 *Phys. Rep.* **309** 211
[48] Hohenberg P and Kohn W 1964 *Phys. Rev.* **136** B864
[49] Kohn W and Sham L J 1965 *Phys. Rev.* **140** A1133
[50] Ceperley D M and Alder B I 1980 *Phys. Rev. Lett.* **45** 566
[51] Perdew J and Zunger A 1981 *Phys. Rev.* B **23** 5048
[52] Kleinman L and Bylander D M 1982 *Phys. Rev. Lett.* **48** 1425
[53] Hamann D R, Schlüter M and Chiang C 1979 *Phys. Rev. Lett.* **43** 1494
[54] Troullier N and Martins J L 1991 *Phys. Rev.* B **43** 1993
[55] Louie S J, Froyen A and Cohen M L 1982 *Phys. Rev.* B **26** 1738
[56] Perdew J P and Wang Y 1992 *Phys. Rev.* B **45** 13 244